Prediction of the Structural Stiffness of Bump-Type Gas Foil Bearings.

Ashutosh Kharche,Biren Kumar Pradhan, Debanshu S Khamari,Suraj Kumar Behera

National Institute of Technology,Rourkela,Rourkela -769008,Odisha,India.

ABSTRACT

Gas bearings are preferable for contamination free high-speed application such as turbo-expanders, air cycle machine, turbo-compressors, etc. The major issue with gas bearings is its low dynamic coefficients such as stiffness and damping due to the low viscosity of the bearings gases. Low stiffness and damping are the major reasons for rotor instability at high-speed operation. The stiffness of a gas bearing can be tailored by use of spring-like foil structure as in gas foil bearings (GFBs). In comparison with other GFBs such as tape and leaf type, bump type GFBs are more popular among tribologists due to its ease of fabrication and assembly. The stiffness of bump type GFBs is controlled by the stiffness of smooth top foil, pressurized gas, and the bump foils. The bump stiffness predominates among three for the overall stiffness of a gas foil bearing. In gas foil bearings, the foils are very thin of the order 0.1 mm, so prediction of structural stiffness is a challenging task for researchers. Current paper explains about a detailed prediction methodology for structural stiffness of a single bump considering friction with its adjacent structures such as top foil and bearing base. The strain energy of simply supported single bump foil is determined and castigliano's theorem is used to predict the stiffness. The behaviors of structural stiffness are further studied with various geometrical parameters of the bump foil and compared with models from literature**.**

Keywords: *Gas Foil Bearings, Bump Foil, Structural Stiffness.*

1.Introduction

Gas bearings are one of the most preferred options for high-speed and contamination free application such as cryogenic turbo-expander. The gases, unlike liquid lubricated bearings, have low viscosity, which leads to low stiffness and damping. Stiffness and damping are being dynamics coefficients of any rotor-bearings system. So low stiffness and damping lead to dynamic instability of rotor-bearings systems at high operational speed. Complaint gas bearings (GFBs) are suitable for such high rotational speed application as it has the ability to tailor its damping and stiffness coefficient by modifying the geometrical and material.

A compliant gas bearing such as gas foil bearing (GFB) comprises a top foil, which is being supported by an elastic foundation. The elastic foundation contains several spring-like beds such as corrugated sub-foils. These sub foils are generally thin and expandable membrane-like structures wrapped around the bearing and termed as bump foil. On the bearing surface, the bumps are arranged in the circumferential direction across the width of the bearing. The geometry of the bump strips may vary from one to another. Current research targets to predict the structural stiffness of gas foil bump type bearing.

Various models have been proposed for the investigation of the structural stiffness of the bump foil. The first attempt is made by walowit and anno, they developed a relation to calculate static stiffness of an isolated bump [Walowit J.,Anno J.,1985]. The friction between the bump foil and the substrate is considered while friction between bump foil and the top foil is neglected. The another model is developed by Heshmat in 1983, this model is still attractive and was used by Peng and Khonsari[Peng, Z. C., and Khonsari,2004]. In 1996 Iordanoff proposed a model which can be used for both the end conditions such as fixed- fixed and free-free. Iordanoff considers the friction between bump foil and bearing base as well as between bump foil and top foil [Iordanoff, I., 1999]. Although these models do not exactly express the real conditions but it gives fair results.

Heshmat tested the complete bearing with multistage bump foil used at static load and zero rotational speed. Stiffness can be varying by using staggered bumps.It increases with increase in load. This feature is again used in series of experiments. Current work explains about a detailed prediction methodology for structural stiffness of a single bump considering friction with its adjacent structures such as top foil and bearing base and the interaction between the adjacent bumps.

1.1. Working principle of bump type gas foil bearing

The generated pressure profile due to wedging action inside the bearing, over the bearing surface, exerts a varying load on the top foil. Eventually, the load is transmitted to the elastic foundation and finally to the bearing base. The exerted load compresses the sub foil radially, which causes the bump foil to expand in the circumferential direction. During the transmission of forces, energy is dissipated because of Coulomb's friction. The Coulomb's friction usually occurs between the top foil, elastic foundation and the bearing base. These subsequent phenomena produce damping inside the bearing. The dissipation of more energy due to Coulomb's friction can enhance the effective damping

of the GFB. In other words, the frictional forces restrict the bump foil expansion in the circumferential direction and enhance the stiffness in the radial direction. For better governing of stability and rotordynamic analysis predicting structural stiffness of bump foil is essential.
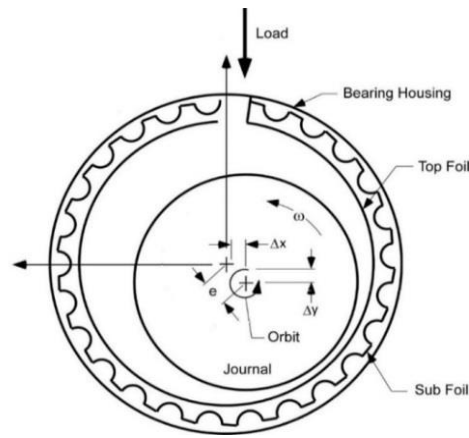

Fig. 1- Schematic view of a typical GFB [Biren Kumar Pradhan,2017]

2.Methodology

A single bump foil is modelled considering the aerodynamic pressure, various reaction forces from adjacent bump foil, friction between the bump-top foil and between bump-bearing bases. The predicted stiffness is compared with the Iordanoff's formulae for free bumps. The Iordanoff's formula is given in Eq. 1[Iordanoff, I., 1999].

In Iordanoff's formulae, the structural stiffness is calculated considering the influence of each bump, the radial position of the applied load and dry friction coefficient between the bump and bearing base. Following assumptions are made in the formulation of the formula [Iordanoff, I., 1999].
- The bump material is isotropic.
- The pitch between bumps is constant.
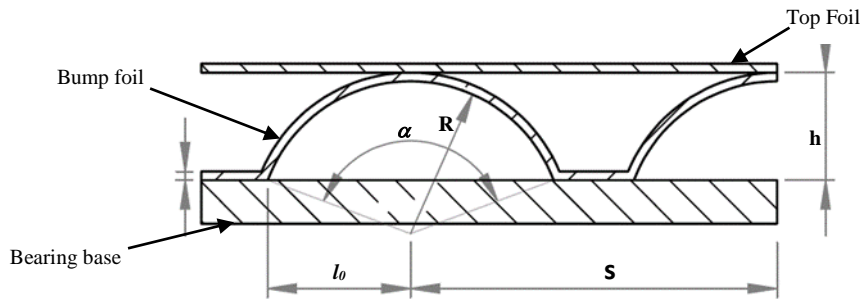- The interaction between bumps is neglected.

Fig.2-Bump geometric parameters for bump stiffness calculation[Iordanoff, I., 1999]

The stiffness, K_{bump} for a single bump with free ends condition, is given in Eq. (1). The total stiffness of bump foil is a number of bumps times K_{bump} [Iordanoff, I., 1999]

$$K_{bump} = \frac{ELt_b^3 \sin^3(\alpha/2)}{6l_0(1-\nu^2)}\left(\frac{1}{I(\alpha,\mu_f)}\right)$$

(1)

Where, $L = \dfrac{Axial\,length\,of\,foil\,bearing}{No\,of\,bump\,strips}$ and $\mu_f = \begin{pmatrix} Dry\,friction\,coefficient \\ between\,elastic\,foundation \\ and\,bearing\,base \end{pmatrix}$

$$I(\alpha,\mu_f) = \left(A^2 + \frac{1+\mu_f^2}{2}\right)\frac{\alpha}{2} - \left(\frac{1-\mu_f^2}{4}\right)\sin\alpha - \frac{\mu_f}{2}(\cos\alpha - 1) - 2A\left(1 - \cos\left(\frac{\alpha}{2}\right) + \mu_f \sin\alpha\right)$$

$$A = \sin\left(\frac{\alpha}{2}\right) + \mu_f \cos\left(\frac{\alpha}{2}\right)$$

According to Walowit's model Bump stiffness is given as in eq. (2).

$$K_{bump} = \frac{ELt_b^3}{2l_b^3\left(1-\nu^2\right)} \tag{2}$$

2.1 Modelling of single bump foil

List of Assumptions for present work is provided below

- The bump material is homogenous.
- The bump foil geometry is uniform throughout the foil.
- Obliquities are neglected.
- The elastic foundation does not detach from the bearing base.
- The effect of the flat portion (Section BB_1 and AA_1 in Fig.) has been considered.
- The bump foils are free to slide over each other and over bearing surface.
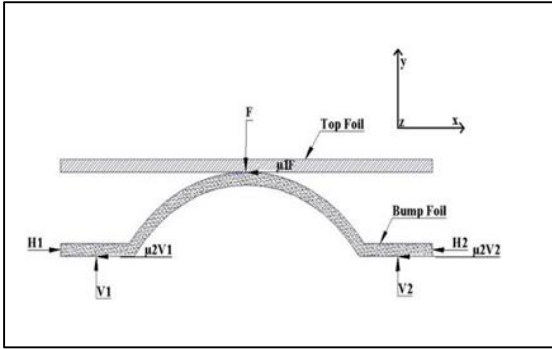- The effect of top foil has been considered for analysis.

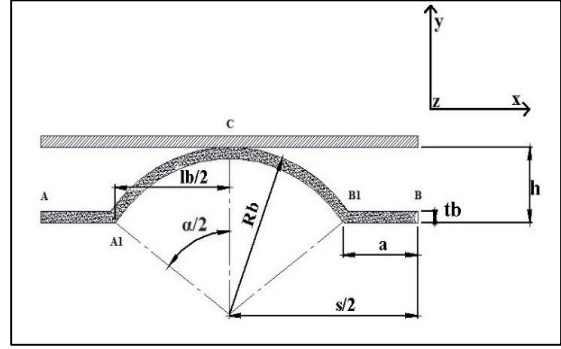Fig. 3 -Free body diagram of a single bump foil

Fig. 4 -Nomenclature of a single bump foil

Castigliano's theorem states that the partial differentiation of strain energy with respect to a generalised force provides the deflection acting along the direction of the force at the point of action. From the list of assumptions, it can be concluded that, at the point of contact between the elastic foundation and the bearing base, the deflection is zero. Hence, from Castigliano's theorem, it can be said that the partial differentiation of strain energy with respect to contact forces (V_1 and V_2).

2.2 FBD Analysis

Bump foil is assumed to be in equilibrium (Both translational and rotational). Hence, the summation of forces and moments must be equal to zero. Mathematically this can be represented as

$$\sum F_x = 0 \,,\, \sum F_y = 0 \text{ and } \sum M_z = 0 \tag{3}$$

`Now, for mathematical analysis, all the unknown forces should be calculated. There are four unknown forces i.e. $\left(V_1, V_2, H_1 \text{ and } H_2\right)$. In contrary, only three equations are available. Compatibility equation is used to solve for the unknown. As per assumptions provided earlier, that the contact force between bearing base and bump foil can never be zero. Hence, this can be written as

$$\frac{\partial U}{\partial V_i} = 0 \qquad \text{Where, } i = 1 \text{ and } 2 \tag{4}$$

Where, U = Strain energy of a single bump (AA_1CB_1B of Fig. 4)

The deflection due to force V can be assumed zero. If the above condition is not satisfied, the bump foil will detach from the bearing base. For the calculation of strain energy, the geometric and elastic constants to be required and they are described in nomenclature section.

Table 1-Nomenclature

Symbols	Description	Symbols	Description

F	Force from top foil to bump foil due to the aerodynamic pressure	t_b	Thickness of bump foil
V_1	Normal force on the bump foil from bearing base on the bump foil (Left Side)	R_b	Radius of the bump
V_2	Normal force on the bump foil from bearing base on the bump foil (Right Side)	h	Bump height
H_1	Force applied on the bump foil from the left-side bump foil	s	Bump pitch
H_2	Force applied on the bump foil from the right-side bump foil	l_b	Bump length
$\mu_1 F$	Friction force on the bump foil due to the top foil	l	Length of bump foil in Z-direction
$\mu_2 V_1$	Friction force on the bump foil due to bearing base on the left-side	a	$\dfrac{(s - l_b)}{2}$
$\mu_2 V_2$	Friction force on the bump foil due to bearing base on the right-side	A	Transverse area of the cross section $= l \times t_b$
E	Young's Modulus of Elasticity	I	Area moment of inertia (Transverse) $= \dfrac{l \times t_b^{3}}{12}$
G	Modulus of Rigidity	α	Bump angle $= 2\sin^{-1}\left(\dfrac{l_b}{2R_b}\right)$
A_0	Area of the flat surface in contact with bearing base $= (a \times l)$	U	Strain energy of a single bump foil
ν	Poisson's Ratio	μ_1	Coefficient of friction between top foil and bump foil
D	Flexural rigidity of top foil $= \dfrac{Et_b^{3}}{12(1 - \nu^2)}$	μ_2 .	Coefficient of friction between bump foil and bearing base
M	Bending Moment	δ	Deflection of Bump foil
K	Stiffness of Bump foil	l0	Half bump length

2.3 Determination of the strain energy of a single bump foil

The strain energy for sections BB_1, B_1C, AA_1 and A_1C are formulated in subsequent subsections. The component of forces utilised to formulate the strain energy is shown in Fig. 5 and Fig. 6. The forces acting on the section AA_1 and B_1C are similar with forces acting on BB_1 and A_1C respectively.
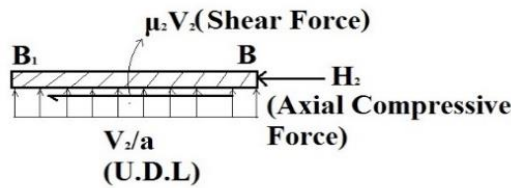

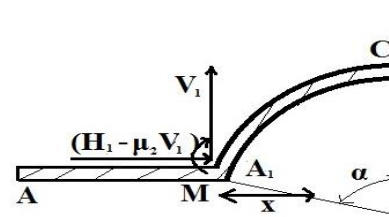**Fig. 5 -Show a figure with all forces acting on section BB1**

Fig. 6 -Show a figure with components of forces for section A₁C

Strain energy of section BB_1 (U_{BB_1})

The strain energy over section BB_1 is a summation of strain energy due to Bending Moment (M_z), strain energy due to axial force (H_2), strain energy due to shear force $(\mu_2 V_2)$ and strain energy due to shear force (V_2). The strain energy U_{BB_1} is represented as in Eqn. (5)

$$U_{BB_1} = \int_0^a \left(\frac{M_z^2}{2EI}\right)dx + \int_0^a \left(\frac{H_2^2}{2AE}\right)dx + \int_0^{t_b} \left(\frac{(\mu_2 V_2)^2}{2A_0 G}\right)dy + \int_0^a \frac{\left(\left(\frac{V_2}{a}\right)x\right)^2}{2AG}dx \tag{5}$$

Bending moment (M_{z_x}) at any distance x from the right end of (B) (Fig. 5) can be given by Eqn. (6)

$$M_z(x) = \left(\frac{V_2}{a}\right)\frac{x^2}{2} \tag{6}$$

Vertical force (V_2) over B_1B, which is distributive contact force, is assumed uniform in nature. Hence, force per unit length can be given as $\left(\frac{V_2}{a}\right)$.

Substituting the parameters M_z, I, A, A_0 and G in the Eqn. (5) and integrating, the equation is rewritten as in Eqn. (7).

$$U_{B_1B} = \left(\frac{V_2^2}{2AE}\right)\left[\left(\frac{3}{5}\right)\left(\frac{a}{t_b}\right)^2 + 2\mu_2^2(1+v)\left(\frac{t_b}{a}\right)^2 + \left(\frac{H_2^2}{V_2^2}\right) + \frac{2(1+v)}{3}\right] \tag{7}$$

Strain energy of section B_1C (U_{B_1C})

$$U_{B_1C} = \int_0^{\alpha/2}\left(\frac{M_z^2}{2EI}\right)R_b d\theta + \int_0^{\alpha/2}\left(\frac{F_1^2}{2EA}\right)R_b d\theta + \int_0^{\alpha/2}\left(\frac{F_2^2}{2GA}\right)R_b d\theta \tag{8}$$

Where,

$$M_z(\theta) = V_2\left(\frac{a}{2} + \frac{l_b}{2} - R_b\sin\left(\frac{\alpha}{2}-\theta\right)\right) - (H_2 + \mu_2 V_2)\left(h + R_b\left(\cos\left(\frac{\alpha}{2}-\theta\right)-1\right)\right)$$

$$F_1 = V_2\sin\left(\frac{\alpha}{2}-\theta\right) + (H_2 + \mu_2 V_2)\cos\left(\frac{\alpha}{2}-\theta\right) \quad , \quad F_2 = V_2\cos\left(\frac{\alpha}{2}-\theta\right) - (H_2 + \mu_2 V_2)\sin\left(\frac{\alpha}{2}-\theta\right)$$

Similarly, U_{AA_1}, U_{A_1C} can be calculated.

The strain energy of a single bump is

$$U = U_{AA_1} + U_{A_1C} + U_{B_1C} + U_{BB_1} \tag{9}$$

2.4 Determination of the unknown forces

Using equilibrium Eq. (3),

$$H_1 = H_2 + \mu_2(V_1 + V_2) + \mu_1 F \qquad F = V_1 + V_2 \qquad V_1\frac{(a+l_b)}{2} - H_1 h + \mu_2 V_1 h - V_2\frac{(a+l_b)}{2} + H_2 h + \mu_2 V_2 h = 0 \tag{10}$$

Solving for equation Eqn. (10), V_1 and V_2 can be expressed as a function of F

$$V_1 = F\left(\frac{1}{2} + \frac{2\mu_1 h}{a+l_b}\right) \text{ and } V_2 = F\left(\frac{1}{2} - \frac{2\mu_1 h}{a+l_b}\right) \tag{11}$$

Eqn. (11) can be re-written by substituting expression for U and V_1 as in Eqn. (12)

$$\frac{V_1 a}{AE}\Delta_1 + \frac{V_1 R_b}{EI}\Delta_2 - \frac{\mu_2 R_b(H_1 - \mu_2 V_1)}{EI}\Delta_3 - \frac{R_b(H_1 - 2\mu_2 V_1)}{EI}\Delta_4 + \frac{V_1 R_b}{4AE}(\alpha - \sin\alpha) - \frac{\mu_2 R_b(H_1 - \mu_2 V_1)}{4AE}(\alpha + \sin\alpha) + \frac{R_b(H_1 - 2\mu_2 V_1)}{4AE}(1 - \cos\alpha)$$

$$+\frac{V_1 R_b}{4AG}(\alpha + \sin\alpha) - \frac{\mu_2 R_b(H_1 - \mu_2 V_1)}{4AG}(\alpha - \sin\alpha) - \frac{R_b(H_1 - 2\mu_2 V_1)}{4AG}(1 - \cos\alpha) = 0 \tag{12}$$

Rearranging the Eqn. (12), the unknown force H_1 is determined as in Eqn. (13)

$$H_1 = F\zeta_3 \tag{13}$$

Where,

$$\zeta_3 = \zeta_1\frac{\Delta_5}{\Delta_6} \ , \ \zeta_1 = \left(\frac{1}{2} + \frac{2\mu_1 h}{a+l_b}\right), \ \Delta_1 = \left(\frac{3}{5}\right)\left(\frac{a}{t_b}\right)^2 + 2\mu_2^2(1+v)\left(\frac{t_b}{a}\right)^2 + \frac{2(1+v)}{3}$$

$$\Delta_2 = \frac{R_b^2}{4}(\alpha - \sin\alpha) + (a+l_b)^2\left(\frac{\alpha}{8}\right) - R_b(a+l_b)\left(1 - \cos\frac{\alpha}{2}\right) \qquad \Delta_3 = R_b^2\left(\frac{3\alpha}{4} - 2\sin\frac{\alpha}{2} + \sin\frac{\alpha}{4}\right) + h^2\frac{\alpha}{2} - 2R_b h\left(\frac{\alpha}{2} - \sin\frac{\alpha}{2}\right)$$

$$\Delta_4 = R_b{}^2\left(\frac{\cos\alpha}{4} - \cos\frac{\alpha}{2} + \frac{3}{4}\right) + R_b\left(\frac{a+l_b}{2}\right)\left(\sin\frac{\alpha}{2} - \frac{\alpha}{2}\right) + h\left(\frac{a+l_b}{2}\right)\frac{\alpha}{2} - R_b h\left(1 - \cos\frac{\alpha}{2}\right)$$

$$\Delta_5 = \Delta_1\frac{a}{R_b} + \Delta_2\frac{A}{I} + \mu_2^2\Delta_3\frac{A}{I} + 2\mu_2\Delta_4\frac{A}{I} + \frac{(\alpha-\sin\alpha)}{4} + \frac{\mu_2^2(\alpha+\sin\alpha)}{4} - \frac{\mu_2}{2}(1-\cos\alpha) + (1+v)\left(\frac{\alpha+\sin\alpha}{2} + \frac{\mu_2^2(\alpha-\sin\alpha)}{2} + \mu_2(1-\cos\alpha)\right)$$

$$\Delta_6 = \mu_2\Delta_3\left(\frac{A}{I}\right) + \Delta_4\left(\frac{A}{I}\right) + \frac{\mu_2(\alpha+\sin\alpha)}{4} - \frac{1-\cos\alpha}{4} + \frac{\mu_2(1+v)}{2}(\alpha-\sin\alpha) + \frac{(1+v)}{2}(1-\cos\alpha)$$

Similarly, from $\dfrac{\partial U}{\partial V_2} = 0$ $\qquad\qquad\qquad\qquad$ $H_2 = F\zeta_4$ $\qquad\qquad\qquad$ (14)

Where,

$$\zeta_4 = \zeta_2\frac{\Delta_7}{\Delta_8} \quad , \qquad \zeta_2 = \left(\frac{1}{2} - \frac{2\mu_1 h}{a+l_b}\right)$$

$$\Delta_7 = \Delta_1\frac{a}{R_b} + \Delta_2\frac{A}{I} + \mu_2^2\Delta_3\frac{A}{I} - 2\mu_2\Delta_4\frac{A}{I} + \frac{(\alpha-\sin\alpha)}{4} + \frac{\mu_2^2(\alpha+\sin\alpha)}{4} + \frac{\mu_2}{2}(1-\cos\alpha) + (1+v)\left(\frac{\alpha+\sin\alpha}{2} + \frac{\mu_2^2(\alpha-\sin\alpha)}{2} - \mu_2(1-\cos\alpha)\right)$$

$$\Delta_8 = -\mu_2\Delta_3\left(\frac{A}{I}\right) + \Delta_4\left(\frac{A}{I}\right) - \frac{\mu_2(\alpha+\sin\alpha)}{4} - \frac{1-\cos\alpha}{4} - \frac{\mu_2(1+v)}{2}(\alpha-\sin\alpha) + \frac{(1+v)}{2}(1-\cos\alpha)$$

2.5 Determination deflection and structural stiffness

The total strain energy in terms of F can be represented as:

$$U = F^2\psi$$

Where, $\psi = \psi_1 + \psi_2 + \psi_3 + \psi_4 + \psi_5 + \psi_6 + \psi_7 + \psi_8$

$$\psi_1 = \frac{\zeta_1^2 a}{2AE}\left(\Delta_1 + \left(\frac{\zeta_3}{\zeta_1}\right)^2\right) , \qquad \psi_2 = \frac{R_b}{2EI}\left(\Delta_2\zeta_1^2 + \Delta_3(\zeta_3 - \mu_2\zeta_1)^2 - 2\Delta_4\zeta_1(\zeta_3 - \mu_2\zeta_1)\right)$$

$$\psi_3 = \frac{R_b}{2AE}\left(\frac{\zeta_1^2}{4}(\alpha-\sin\alpha) + \frac{(\zeta_3 - \mu_2\zeta_1)^2}{4}(\alpha+\sin\alpha) + \frac{\zeta_1(\zeta_3 - \mu_2\zeta_1)}{2}(1-\cos\alpha)\right)$$

$$\psi_4 = \frac{\zeta_2^2 a}{2AE}\left(\Delta_1 + \left(\frac{\zeta_4}{\zeta_2}\right)^2\right) , \qquad \psi_5 = \frac{R_b}{2EI}\left(\Delta_2\zeta_2^2 + \Delta_3(\zeta_4 + \mu_2\zeta_2)^2 - 2\Delta_4\zeta_2(\zeta_4 + \mu_2\zeta_2)\right)$$

$$\psi_6 = \frac{R_b}{2AE}\left(\frac{\zeta_2^2}{4}(\alpha-\sin\alpha) + \frac{(\zeta_4 + \mu_2\zeta_2)^2}{4}(\alpha+\sin\alpha) + \frac{\zeta_2(\zeta_4 + \mu_2\zeta_2)}{2}(1-\cos\alpha)\right)$$

$$\psi_7 = \frac{R_b(1+v)}{AE}\left(\frac{\zeta_1^2}{4}(\alpha+\sin\alpha) + \frac{(\zeta_3 - \mu_2\zeta_1)^2}{4}(\alpha-\sin\alpha) - \frac{\zeta_1(\zeta_3 - \mu_2\zeta_1)}{2}(1-\cos\alpha)\right)$$

$$\psi_8 = \frac{R_b(1+v)}{AE}\left(\frac{\zeta_2^2}{4}(\alpha+\sin\alpha) + \frac{(\zeta_4 + \mu_2\zeta_2)^2}{4}(\alpha-\sin\alpha) - \frac{\zeta_2(\zeta_4 + \mu_2\zeta_2)}{2}(1-\cos\alpha)\right)$$

Now, from Castigliano's Theorem the deflection is found to be:

$$\delta = \frac{\partial U}{\partial F} = 2F\psi \qquad\qquad\qquad\qquad (15)$$

Hence, the structural stiffness of the single bump is found to be:

$$K = \frac{F}{\delta} = \frac{1}{2\psi} \qquad\qquad\qquad\qquad (16)$$

Where, $\psi = f(R_b, l_b, l, t_b, h, s, E, \nu, \mu_1, \mu_2)$

Table 2 - Geometrical parameters and material properties of bump foil

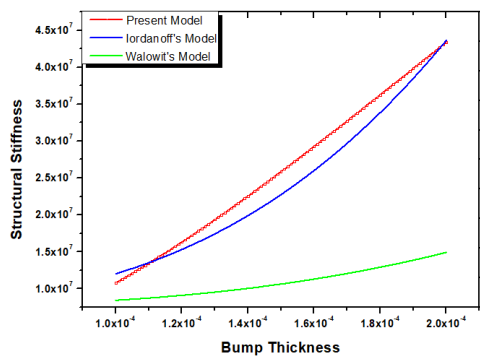| Bump Parameter	Dimension	Bump Parameter	Dimension
Bump Foil Thickness (t_b)	0.10 mm	Bump Foil Material	Phosphor Bronze
Bump Pitch (s)	3.17 mm	Young's Modulus(E)	114 GPa
Bump Length ($2l_b$)	2.36 mm	Poisson's Ratio (ν)	0.38
Bump Height (h)	0.60 mm	Coefficient of Friction (μ_1) (Top Foil-Bump Foil)	0.35
		Coefficient of Friction (μ_2) (Bearing Base-Bump Foil)	0.35

3. Result and Discussion

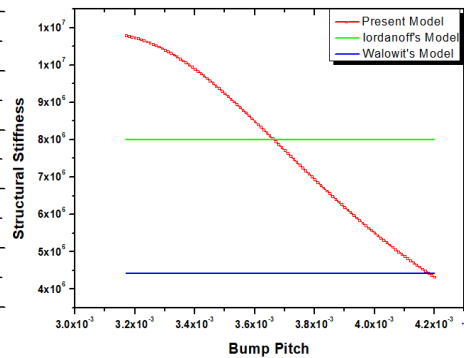Fig. 7 - Variation of Structural stiffness with Bump thickness

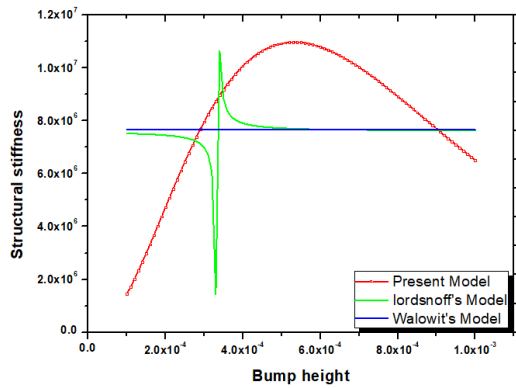Fig. 8 - Variation of Structural stiffness with Bump pitch

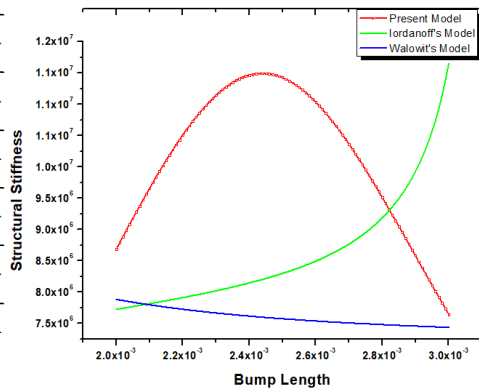Fig. 9 - Variation of Structural stiffness with Bump height

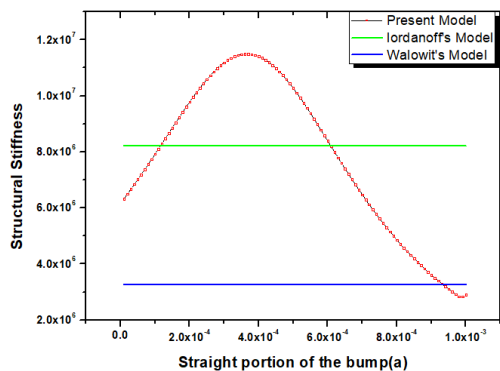Fig.10-Variation of Structural stiffness with Bump length

Fig.11-Variation of Structural stiffness with Straight portion of the Bump foil (a)
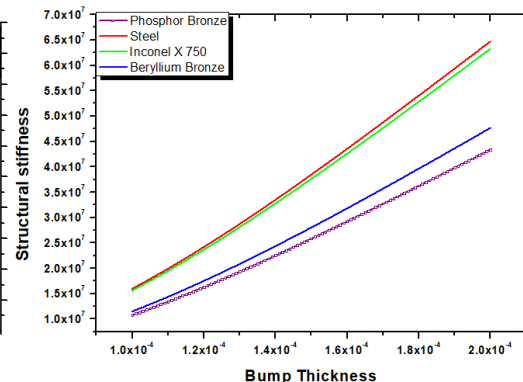

Fig.12-Variation of Structural stiffness with Bump thickness for different Bump material

The present formulation to predict bump stiffness is compared with Iordanoff's formula [Iordanoff, I., 1999]. Curves are drawn to study the prediction of bump stiffness with variation geometrical parameters and different materials such as bump pitch, height, thickness, bump length etc. (7 to 12).

The stiffness is directly proportional to the rigidity of the structure and the rigidity of the structure is directly proportional to the foil thickness. Fig. 7 represents the variation of structural stiffness with bump foil thickness. Both Iordanoff's model and Walowit's model [Walowit J., Anno J.,1985] also show similar as predicted with respect to thickness. The minor deviation is due to the additional boundary conditions incorporated in current methodology.

Fig. 8 represents the variation of structural bump stiffness with Bump pitch. It can be seen from the equation (1) and (2) that the structural stiffness of the bump is independent of the bump pitch and hence both Iordanoff's and Walowit's model shows that the stiffness remains constant with change in pitch. But the proposed model predicts that the stiffness of bump decreases with increase in bump pitch. It is because of decrease in rigidity of the bump foil with increase in pitch.

The variation of stiffness with respect to bump height is presented in Fig.9. It can be observed that the stiffness gives anomalous behaviour at a specific range. Beyond the above range, there is no variation of stiffness, which is quite inconvenient. Again, in case of Walowit's formulae the bump stiffness is constant as the formulae is independent of bump height. The present work shows a smooth variation of stiffness with an optimized value of bump height.

Fig.10 represents the variation of stiffness with bump length with other parameters keeping constant. As per iordanoff's model, the stiffness of bump foil increases with increase in bump length while Walowit's model shows that the stiffness decreases with increase in bump length. The bump length is a function of bump angle and pitch so, proposed model shows that the structural stiffness of bump foil increases up to specific bump length and then starts decreasing.

Fig. 11 shows the variation of structural stiffness with the straight portion of the bump foil. The bump length and the straight portion of the bump foil in contact with the bearing base are directly proportional to each other. In addition, the interaction between the adjacent bumps is considered in this model, which may deflect the straight portion of the bump and changes its stiffness. While in both Iordanoff;s and Walowit's model, the structural stiffness of the bump foil is independent of the straight portion and hence remains constant.

The variation of structural stiffness with respect to bump thickness for different bump foil material is shown in **Error! Reference source not found.**12. Four different materials have been considered i.e. phosphor bronze, steel, Inconel X 750 and beryllium bronze. Variation of stiffness with different elastic properties as well as coefficient of friction have been studied.

4. CONCLUSION

For rotordynamic analysis of the bearing system, bearing stiffness and damping coefficients are essential. For GFBs the bearing stiffness depends on air stiffness, top foil stiffness and bump foil stiffness. The structural stiffness of the bump foil and top foil is constant. In contrary, the air stiffness varies with the aerodynamic pressure profile. In the present work, the bump stiffness is predicted and compared with analytical Iordanoff's formulation [Iordanoff, I., 1999]. Following conclusion can be drawn after detailed analysis.

- With the increase in pitch(s) and bump length(l_b), the structural stiffness of the bump foil decreases significantly. In contrary, with an increase in thickness(t_b), the bump stiffness increases radically.

- The formulae developed in current research for structural stiffness of a single bump foil provides more convenient results to predict the change in structural stiffnes of the bump foil with change in geometrical and material properties of the foil than both Walowit's model [Walowit J.,Anno J.,1985] and Iordanoff's model [Iordanoff, I., 1999].

REFERENCES

Biren Kumar Pradhan, 2017, " Static and Dynamic Analysis of Gas Foil Journal Bearing for High-Speed Rotor,"M. Tech. dissertation, NIT Rourkela.

Walowit J. A. and Anno J. N., 1975, Modern Developments in Lubrication Mechanics, *Applied Science Publishers, Ltd., Landon.*

Iordanoff, I., 1999, Analysis of an Aerodynamic Compliant Foil Thrust Bearing: Method for a Rapid Design, *ASME J., Tribol., 121. pp.816-822.*

Le Lez, S., Arghir, M., and Frene, J., 2007, "A New Bump-Type Foil Bearing Structure Analytical Model," *ASME J. Eng. Gas Turbines Power*, 129_4_, pp.1047–1057.

Ku, C.-P. R. and Heshmat, H., Compliant Foil Bearing Structural Stiffness Analysis Part I: Theoretical Model-Including Strip and Variable Bump Foil Geometry, *ASME Jour. of Teb., 114, 2, pp 394-400, (1992).*

Peng, Z. C., and Khonsari, M. M., 2004, Hydrodynamic Analysis of Compliant Foil Air Bearings with Compressible Air Flow, *ASME J. Tribol., 126, pp. 542–546.*